Smart Mater. Struct. **17** (2008) 045001 (5pp) doi:10.1088/0964-1726/17/4/045001

# Analysis and fabrication of patterned magnetorheological elastomers

**Xianzhou Zhang**[1], **Suili Peng**[2], **Weijia Wen**[2] **and Weihua Li**[1,3]

[1] School of Mechanical, Materials and Mechatronic Engineering, University of Wollongong, Wollongong, NSW 2522, Australia
[2] Institute of Nano Science and Technology, Department of Physics, The Hong Kong University of Science and Technology, Clear Water Bay, Kowloon, Hong Kong, People's Republic of China

E-mail: weihuali@uow.edu.au

Received 6 January 2008, in final form 9 April 2008
Published 20 May 2008
Online at stacks.iop.org/SMS/17/045001

**Abstract**
This paper presents analysis, fabrication and characterization of patterned magnetorheological (MR) elastomers. By taking into account the local magnetic field in MREs and particle interaction magnetic energy, the magnetic-field-dependent mechanical properties of MREs with lattice and BCC structures were theoretically analyzed and numerically simulated. Soft magnetic particles were assembled in a polydimethylsiloxane (PDMS) matrix to fabricate new MR elastomers with uniform lattice and BCC structures, which were observed by a microscope. The field-dependent moduli of the new MR elastomers were characterized by using a parallel-plate MR rheometer. The experimental results agreed well with numerical simulations.

(Some figures in this article are in colour only in the electronic version)

## 1. Introduction

Magnetorheological (MR) materials, including MR fluids, MR foams and MR elastomers, are an important branch of smart materials [1]. For the past two decades, MR fluids have received considerable attention and a variety of applications have been reported [2–5]. MR elastomers (MREs) are composites where highly elastic polymer matrices are filled with magnetic particles. MREs and MR fluids have similar field response properties; however, there are some distinct differences in operating these two classes of materials. The most noteworthy is that MREs operate within the pre-yield regime while MR fluids typically operate in a post-yield continuous shear or flow regime. In other words, the 'strength' of MR fluids is characterized by the yield stress while MREs are characterized by the field-dependent modulus. In view of these applications, MRE devices are used to adjust the natural frequency of a structure, which is dominated by the equivalent stiffness, while MR fluid devices provide a damping function, which is the process of dissipating energy. Therefore, these two materials are complementary rather than competitive. Recently, MREs have found a lot of applications, such as vibration absorbers, engine mounts and variable impedance surfaces [6, 7].

In the literature, both anisotropic [8, 9] and isotropic [10, 11] MREs were fabricated and their mechanical properties have been investigated analytically and experimentally. In analyzing the field-dependent modulus of MREs, a number of models were proposed based on the analysis of the dipole model for particle energy interaction. Jolly *et al* [12] presented a point-dipole model, where the MR effect was studied as a function of particle magnetization. This model was borrowed from the previous studies on MR fluids. Davis [13] calculated the shear increment by using finite element analysis, which was for isolated single chains of periodically spaced dipoles. Shen *et al* [14] fabricated MREs with polyurethane and a natural rubber matrix and presented a mathematical model to represent the stress–strain relationship of MRE. This model takes into account all the dipole interactions in a chain. Zhang *et al* [15] proposed a model by considering the local field. It is noted that these modeling studies are based on the assumption that MREs only have a simple chain structure, where all particles are located within chains. There are very few reports discussing the influence of other chains and in predicting the field-dependent properties with other complex structures. This may be due

[3] Author to whom any correspondence should be addressed.

 

to the fact that it is difficult to find an effective fabrication technique in developing MREs with precisely controlled structures. Also, the modeling approach to the field-dependent properties of MREs with complex structures is very rare. This is the motivation of this research.

This paper consists of two major parts. The first part is to theoretically analyze the field-dependent properties of MREs with a pre-designed structure, where both the local magnetic field in MREs and particle interaction magnetic energy will be used to numerically derive the magnetic-field-dependent mechanical properties. The second part is to fabricate MREs with pre-designed structures by using microtechnology and to characterize their field-dependent mechanical properties.

## 2. The simulation analysis of patterned MRE

In this paper, a lattice structure based MRE is first proposed to introduce the simulation approach. As shown in figure 1, the proposed lattice structure MREs consist of $m$ layers, in which the distances of the particles in each layer in three directions are $\mathrm{d}x$, $\mathrm{d}y$ and $\mathrm{d}z$, respectively. Two steps are used to calculate the magnetic energy and field-dependent modulus of the MREs. The first is to calculate the local magnetic field, which is induced by the external magnetic field as well as the dipole fields from all the magnetized particles. The magnetic dipole of particles can be determined by the local field. The second is to represent the interaction energy of a particle with all other particles in the structure. The magnetic-field-induced shear stress can be derived by taking the derivative of interparticle energy density with respect to the scalar shear strain. The field-dependent modulus can be obtained as a consequence. The lattice structure is only used to introduce the calculation method. For the BCC structure, the difference is only in coordinate locations of the particles. The calculation method is the same as that used in the lattice structure. Also, the simple cubic structure is a special case of lattice structure, which has the same side length value in the $x$, $y$ and $z$ axes.

### 2.1. Local magnetic field and magnetic dipole

When a magnetic field $H_0$ is applied to the suspension, the magnetic dipole moment induced on a particle is

$$\mathbf{m}_i = 3\frac{\mu_\mathrm{p} - \mu_\mathrm{m}}{\mu_\mathrm{p} + 2\mu_\mathrm{m}} V_\mathrm{p} H_\mathrm{loc} \tag{1}$$

where $\mu_0$ is the vacuum permeability, $\mu_\mathrm{p}$ is the relative permeability of particles, $\mu_\mathrm{m}$ is the relative permeability of the medium and $V_\mathrm{p}$ is the volume of the particle. The local magnetic field is given by

$$H_\mathrm{loc} = H_0 + H_\mathrm{p} \tag{2}$$

where $H_0$ is the initial magnetic field and $H_\mathrm{p}$ is the magnetic field caused by the dipole moment of all particles.

As shown in figure 1, suppose that the magnetic field is applied in the direction of the $Z$ axis. Also, all the magnetizable particles have been magnetized as dipoles. A magnetic vector potential $A$ at the zero point induced by the magnetic dipole moment $\mathbf{m}$ at position $P(x, y, z)$ can be expressed as

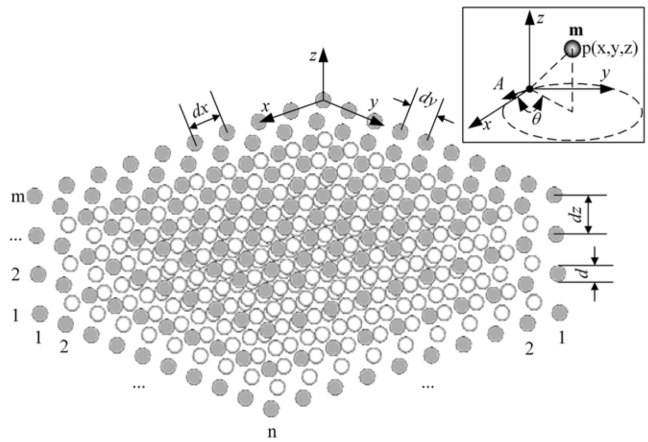


**Figure 1.** Schematic of MREs with a lattice structure and the magnetic field induced by a dipole.

$$\begin{aligned} A_x &= A\sin\theta = \frac{\mu_0}{4\pi}\cdot\frac{y}{(x^2+y^2+z^2)^{3/2}}|\mathbf{m}| \\ A_y &= -A\cos\theta = \frac{\mu_0}{4\pi}\cdot\frac{-x}{(x^2+y^2+z^2)^{3/2}}|\mathbf{m}| \\ A_z &= 0 \end{aligned} \tag{3}$$

where $\sin\theta = y/\sqrt{x^2+y^2}$, $\cos\theta = x/\sqrt{x^2+y^2}$.

For $B = \nabla \times A$

$$\begin{aligned} B_x &= \frac{\mu_0}{4\pi}\cdot\frac{-3xy}{(x^2+y^2+z^2)^{5/2}}|\mathbf{m}| \\ B_y &= \frac{\mu_0}{4\pi}\cdot\frac{-3yz}{(x^2+y^2+z^2)^{5/2}}|\mathbf{m}| \\ B_z &= \frac{\mu_0}{4\pi}\cdot\frac{x^2+y^2+2z^2}{(x^2+y^2+z^2)^{5/2}}|\mathbf{m}| \end{aligned}$$

$$B = B_x i + B_y j + B_z k \qquad \text{and} \qquad H_\mathrm{p} = \sum_{i=1}^{\infty}\frac{B_i}{\mu_0} = D\mathbf{m}, \tag{4}$$

where $B_i$ is the magnetic flux density induced by the dipole $i$. $D$ is the influence factor, which can be calculated with the simulation.

The magnetic dipole moment induced on a particle is

$$\mathbf{m}_i = \frac{3\beta V_\mathrm{p}}{1 - 3D\beta V_\mathrm{p}} H_0 \tag{5}$$

where $\beta = (\mu_\mathrm{p} - \mu_\mathrm{m})/(\mu_\mathrm{p} + 2\mu_\mathrm{m})$.

### 2.2. Interaction energy of particles and field-dependent moduli

The interaction energy of two dipoles $\mathbf{m}_1$ and $\mathbf{m}_2$ can be expressed as

$$E_{12} = \frac{\mu_0\mu_\mathrm{m}}{4\pi}\left(\frac{\mathbf{m}_1\cdot\mathbf{m}_2}{r^3} - \frac{3}{r^5}(\mathbf{m}_1\cdot\mathbf{r})(\mathbf{m}_2\cdot\mathbf{r})\right). \tag{6}$$

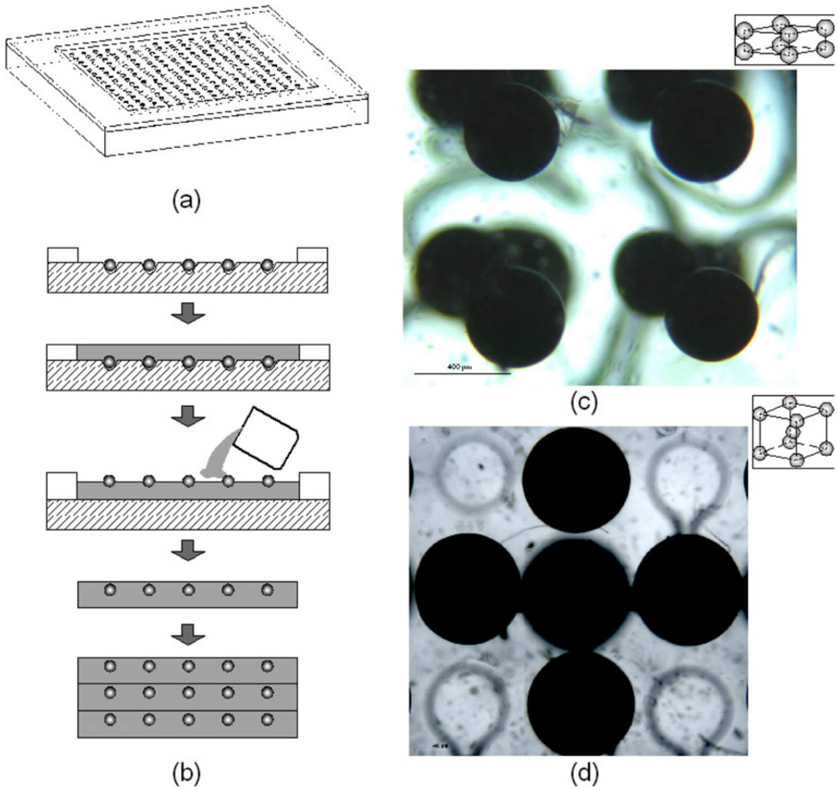


**Figure 2.** The fabrication process of patterned MREs and the sample structures. (a) Patterned mold; (b) fabrication steps; (c) picture of the lattice structure; (d) picture of the BCC structure.

Assuming one dipole is located at the zero point and the other dipole is located at the position $(x, y, z)$, the interaction energy of the two dipoles with equal strength $\mathbf{m}$ and direction is

$$E_{12} = \frac{\mu_0\mu_{\mathrm{m}}|\mathbf{m}|^2}{4\pi}\left(\frac{1-3\cos^2\varphi}{|r|^3}\right) = \frac{|\mathbf{m}|^2\left(1-3\frac{z^2}{x^2+y^2+z^2}\right)}{4\pi\,\mu_0\mu_{\mathrm{m}}(x^2+y^2+z^2)^{3/2}}. \tag{7}$$

For the particle at the coordinate origin, its interaction energy with all the particles is

$$E = \sum_{i=1}^{\infty}\frac{\mu_0\mu_{\mathrm{m}}|\mathbf{m}|^2\left(1-3\frac{z_i^2}{x_i^2+y_i^2+z_i^2}\right)}{4\pi(x_i^2+y_i^2+z_i^2)^{3/2}}. \tag{8}$$

When the particles are moved in the $X$–$Y$ plane (the magnetic field direction is along the $Z$ axis), the interaction energy can be written as

$$E = \sum_{i=1}^{\infty}\frac{\mu_0\mu_{\mathrm{m}}|\mathbf{m}|^2[(x_i+\Delta x_i)^2+(y_i+\Delta y_i)^2-2z_i^2]}{4\pi[(x_i+\Delta x_i)^2+(y_i+\Delta y_i)^2+z_i^2]^{5/2}}. \tag{9}$$

In this paper, only the simple shear in the $x$ direction has been deduced, because the deduction of a 3D shear is too complex in this case. However, for an isotropic structure, the $x$ and $y$ axis shears have the same behaviors. The shear force in any other direction is the combination of the single-direction shears in the $x$ and $y$ axis. By defining the scalar shear strain of the particle chain as $\varepsilon = \frac{\Delta x}{z}$, i.e. the shear direction is in the $x$ axis, the modulus induced by the application of a magnetic field can be computed by taking the derivative of interparticle energy density with respect to the scalar shear strain divided by the shear strain:

$$\Delta G = \sum_{i=1}^{\infty}\left\{3\mu_0\mu_{\mathrm{m}}|\mathbf{m}|^2 z(x_i+\varepsilon z_i)(4z^2-x_i^2-2x_i\varepsilon z_i - \varepsilon^2 z_i^2 - y_i^2)\right\}\left\{4\pi\varepsilon\left(x_i^2+2x_i\varepsilon z_i+\varepsilon^2 z_i^2 + y_i^2+z^2\right)^{7/2}V_{\mathrm{unit}}\right\}^{-1} \tag{10}$$

where $V_{\mathrm{unit}}$ is the unit volume of the structure with one particle. For example, the lattice structure has $V_{\mathrm{unit}} = \mathrm{d}x\,\mathrm{d}y\,\mathrm{d}z$, as shown in figure 1.

## 3. The fabrication of patterned MREs

The matrix for the MRE can be any kind of elastomer, which is used to support the particles but does not react with the MR particles. In this work, polydimethylsiloxane (PDMS) 2025 (Dow Corning 184) material is used as a matrix. This PDMS material is a room-temperature vulcanizing elastomer with a transparent appearance. Pure iron balls, provided by Shenzhen Universal Ball Manufacturing Co. China, were used as dispersed particles.

A schematic diagram of the fabrication process of patterned MREs is shown in figure 2. A patterned mold was prepared at first (figure 2(a)), which is a methyl-methacrylate board with regular holes etched by laser. The pure iron balls

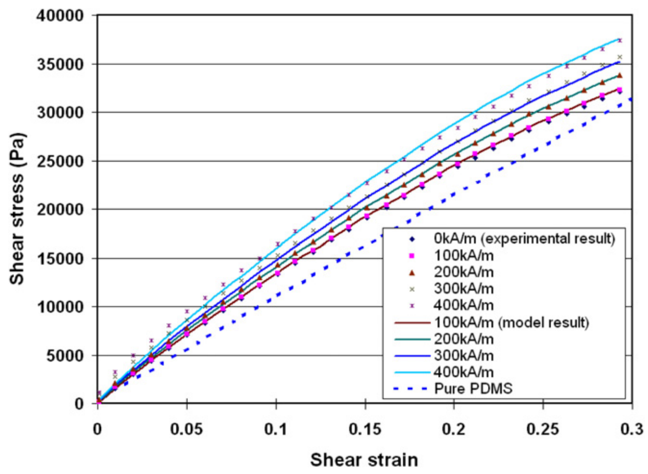


**Figure 3.** The strain–stress curve of lattice structural MRE at different magnetic fields: simulation and experimental results.

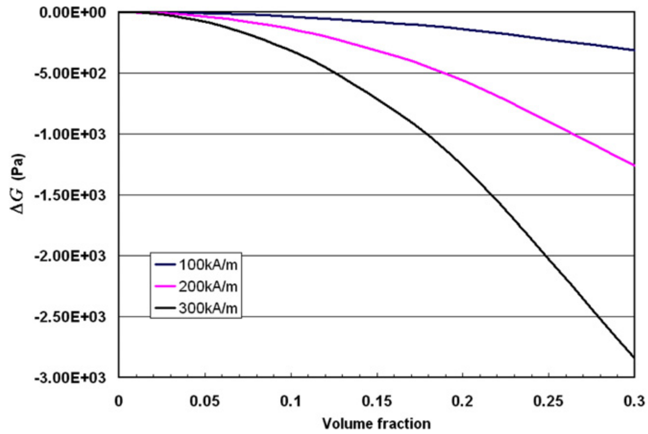


**Figure 4.** The relationship between the field-reduced modulus and particle volume fraction in a BCC MR elastomer.

were filled into the holes of the mold at first. Then a thin layer of PDMS is located on the front surface of the mold, so as to fix the position of the particles. After curing of the PDMS, the thin layer embedded with patterned magnetic iron particles was taken off from the mold. Then we overlap several layers according to the designed position and thickness, and fill the gap with PDMS and remove the air bubbles in a vacuum case. Finally we cure the patterned MRE in a constant temperature oven (figure 2(b)). By using different molds and overlapping positions, different structures of MREs can be obtained, such as lattice chain or body centered tetragonal (BCT). BCT is probably the most stable structure in MR materials. However, in this paper, the body centered cubic (BCC) was selected for study due to its ease of fabrication and simplicity. Different from the BCT structure, which has a field-increasing modulus, the BCC structure has a field-decreasing modulus. This new finding will be discussed in the following calculations and experiments.

Two categories of structures have been fabricated in this work. The first one was the sample with the lattice structure and the second one was the sample with BCC structure, as shown in figures 2(c) and (d), respectively. The photos were taken by a Leica DFC280 microscope. As can be seen from figures 2(c) and (d), the particles are dispersed regularly on the layer. The diameter of the iron ball in sample 1 is 400 $\mu$m, the distance between particles in the plane is 800 $\mu$m and the distance between particles in the thickness direction is 480 $\mu$m. Three layers are prepared in the thickness direction. The parameters in sample 2 are 800 $\mu$m, 1000 $\mu$m and 1000 $\mu$m, respectively.

## 4. Results and discussions

The MR effect of patterned MRE was evaluated by measuring the shear modulus with and without an applied magnetic field using a Physica MRD 180 MagnetoRheological Device (Anton Paar Companies, Germany), equipped with an electromagnet kit. The rubber segments were sandwiched between a rotary disk and a base.

The quasi-static shear mode was employed to evaluate the shear modulus of MRE. Figure 3 shows the strain–stress curves of the lattice structural MRE sample at five different magnetic field intensities of 0, 100, 200, 300 and 400 kA m$^{-1}$, respectively. As can be seen from these figures, the modulus of MREs shows an increasing trend with magnetic field, the properties of which are similar to conventional MREs. The shear stress in the figures is seen as the combination of elastic stress and field-induced stress of the MRE. The simulation result is obtained by the program and the parameters of the sample. Obviously, the model prediction agreed well with experimental results.

In [7], for a chain-like structure-based MRE, the optimum volume fraction of iron particles was predicted to be 27% and the relative change in modulus due to a large magnetic field was approximately 50%. However, our sample has a relatively low modulus increment of 18% in a magnetic field of 400 kA m$^{-1}$, as shown in figure 3. This is mainly due to the fact that the sample has a very low particle volume fraction of 11%. To improve the field-induced modulus, the volume fraction of the particle must be increased.

Using the same theoretical analysis as shown in section 2, the field-dependent modulus change of the BCC-based MRE was calculated by using equation (10). In contrast to the lattice structure MRE, the BCC-based MRE shows a decreasing trend with magnetic field, as shown in figure 4. For example, the modulus change at 300 kA m$^{-1}$ is about two orders higher than that at 100 kA m$^{-1}$. This phenomenon has never been reported in the literature. This finding is very interesting as it may provide a concept to develop 'negative' MREs, which is expected to broaden potential applications of MREs in special conditions. Also, this figure shows that the field-dependent modulus change increases steadily with the increment of particle volume fraction, To verify the simulation analysis, steady shear experiments were conducted and the results were shown in figure 5. It can be seen from this figure that the modulus shows a slightly decreasing trend with magnetic field. It should be noted that the modulus change is not very notable, the reason for which are due to two reasons: one is the particle volume fraction is very low, and the other is the matrix modulus

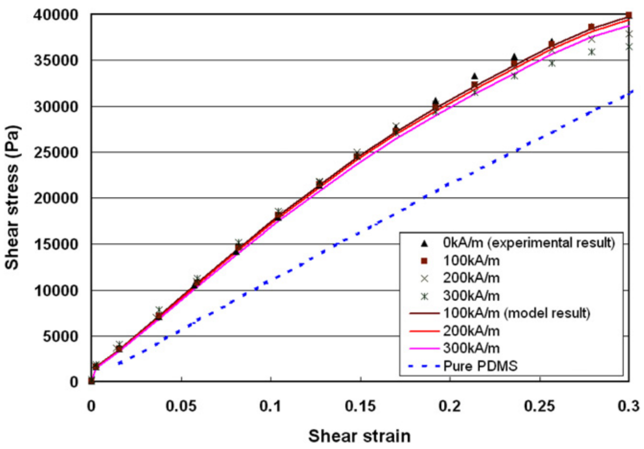


**Figure 5.** The relationship between the shear stress and strain in a BCC MR elastomer.

is quite high. It is noted that the fabricated BCC MREs have limited applications because of very narrow modulus changes. However, these results might provide concepts to develop other new MREs with controllable mechanical properties by designing special patterned structures. In this paper, the shear modulus is derived from the simple shear in one direction and the experimental result is a torsional shear. Although the torsional shear is the combination of the single-direction shears in the $x$ and $y$ axis, and the $x$ and $y$ axis shears have the same behaviors for isotropic structure, there are still some differences. For the lattice structure, the field-dependent modulus is dominated by the particles in one chain and the influence of neighboring chains is relatively low. Thus the difference between torsional shear and single-direction shear can be neglected, and the experimental results are very similar to the simulation results. But for the BCC structure, the influence of neighboring chains is relatively high. This could result in the difference between the experimental and simulation results. In future, a unidirectional shear instrument is needed to be developed to verify the experiments again.

## 5. Conclusions

In this paper, two new MR elastomers, with a lattice structure and a BCC structure, were fabricated by precisely positioning iron particles in a PDMS matrix. Both the MRE samples consist of three layers.

The field-dependent mechanical properties of the patterned MRE were investigated both numerically and experimentally. In numerical analysis, a quasi-static model that examines the effects of magnetic field was presented. This model takes into account the dipole interactions caused by all the dipoles considered, including the local field induced by all the particles and the interaction energy of all the particles. In the experimental approach, the field-dependent modulus was measured under steady shear by using a parallel-plate MR rheometer. For the MRE sample with lattice structure, the relative modulus increment is about 18% at a magnetic field of 400 kA m$^{-1}$. The comparison between experimental results and model predictions indicate that the model could precisely predict material performances. For the MRE sample with a BCC structure, the field-induced modulus shows a decreasing trend with magnetic field, which has never been reported. This study is expected to design and develop novel field-controlled MREs with pre-designed structures.

## References


[1] Carlson J D and Jolly M R 2000 MR fluid, foam and elastomer devices *Mechatronics* **10** 555–69

[2] Nguyen Q, Han Y, Choi S and Wereley N M 2007 Geometry optimization of MR valves constrained in a specific volume using the finite element method *Smart Mater. Struct.* **16** 2242–52

[3] Li W H, Yao G Z, Chen G, Yeo S H and Yap F F 2000 Testing and steady state modeling of a linear MR damper under sinusoidal loading *Smart Mater. Struct.* **9** 95–102

[4] Liu B, Li W H, Kosasih P B and Zhang X Z 2006 Development of an MR-brake-based haptic device *Smart Mater. Struct.* **15** 1960–6

[5] Nguyen Q, Choi S and Wereley N M 2008 Optimal design of magnetorheological valves via a finite element method considering control energy and a time constant *Smart Mater. Struct.* **17** 025024

[6] York D, Wang X and Gordaninejad F 2007 A new MR fluid-elastomer vibration isolator *J. Intell. Mater. Syst. Struct.* **18** 1221–5

[7] Deng H, Gong X and Wang L 2006 Development of an adaptive tuned vibration absorber with magnetorheological elastomer *Smart Mater. Struct.* **15** N111–6

[8] Bellan C and Bossis G 2002 Field dependence of viscoelastic properties of MR elastomers *Int. J. Mod. Phys.* B **16–18** 2447–53

[9] Zhou G Y 2003 Shear properties of a magnetorheological elastomer *Smart Mater. Struct.* **12** 139–46

[10] Lokander M and Stenberg B 2003 Improving the magnetorheological effect in isotropic magnetorheological rubber materials *Polym. Test.* **22** 677–80

[11] Gong X L, Zhang X Z and Zhang P Q 2005 Fabrication and characterization of isotropic magnetorheological elastomers *Polym. Test.* **24** 669–76

[12] Jolly M R, Carlson J D and Munoz B C 1996 A model of the behaviour of magnetorheological materials *Smart Mater. Struct.* **5** 607–14

[13] Davis L C 1999 Model of magnetorheological elastomers *J. Appl. Phys.* **85** 3348–51

[14] Shen Y, Golnaraghi M F and Heppler G R 2004 Experimental research and modeling of magnetorheological elastomers *J. Intell. Mater. Syst. Struct.* **15** 27–35

[15] Zhang X Z, Gong X L, Wang Q M and Zhang P Q 2004 Study on mechanism of squeeze-strengthen effect in magnetorheological fluids *J. Appl. Phys.* **96** 2359–64